Self-Assembly-Induced Far-Red/Near-Infrared Fluorescence Light-Up for Detecting and Visualizing Specific Protein–Peptide Interactions

Huaimin Wang,[†,§] Jie Liu,[‡,§] Aitian Han,[†] Nannan Xiao,[†] Zhaosheng Xue,[‡] Gang Wang,[†] Jiafu Long,[†] Deling Kong,[†] Bin Liu,[‡,*] Zhimou Yang,[†,*] and Dan Ding[†,*]

[†]State Key Laboratory of Medicinal Chemical Biology, Key Laboratory of Bioactive Materials, Ministry of Education, College of Life Sciences, and Collaborative Innovation Center of Chemical Science and Engineering (Tianjin), Nankai University, Tianjin 300071, People's Republic of China, and [‡]Department of Chemical and Biomolecular Engineering, National University of Singapore, 4 Engineering Drive 4, 117576, Singapore. [§]H. Wang and J. Liu contributed equally.

ABSTRACT Understanding specific protein–peptide interactions could offer a deep insight into the development of therapeutics for many human diseases. In this work, we designed and synthesized a far-red/near-infrared (FR/NIR) fluorescence light-up probe (DBT-2EEGWRESAI) by simply integrating two tax-interacting protein-1 (TIP-1)-specific peptide ligands (EEGWRESAI) with one 4,7-di(thiophen-2-yl)-2,1,3-benzothiadiazole (DBT) unit. We first demonstrated that DBT is an environment-sensitive fluorophore with FR/NIR fluorescence due to its strong charge transfer character in the excited state. Thanks to the environmental sensitivity of DBT, the probe DBT-2EEGWRESAI is very weakly fluorescent in aqueous solution but lights up its fluorescence when the probe specifically binds to TIP-1 protein or polyprotein (ULD-TIP-1 tetramer). It is found that the DBT-2EEGWRESAI/TIP-1 protein and the DBT-2EEGWRESAI/ULD-TIP-1 tetramer could self-assemble into spherical nanocomplexes and a nanofiber network, respectively, which lead to probe fluorescence turn-on through providing DBT with a hydrophobic microenvironment. By virtue of the self-assembly-induced FR/NIR fluorescence turn-on, DBT-2EEGWRESAI can detect and visualize specific protein/polyprotein–peptide interactions in both solution and live bacteria in a high contrast and selective manner.

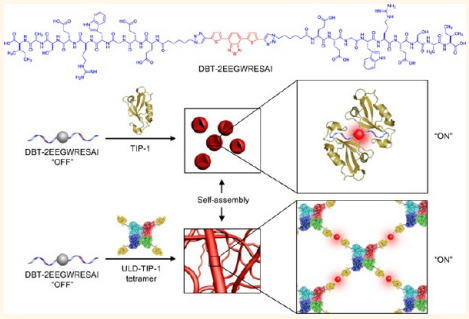

KEYWORDS: protein–peptide interactions · self-assembly · far-red/near-infrared fluorescence · environment-sensitive fluorophore · bacteria

Specific protein–peptide interactions are one of the driving forces inside living cells, which form the basis of many biological processes. Understanding these interactions could offer a deep insight into the development of therapeutics for many human diseases.[1−4] To date, there have been several strategies for studying protein–peptide interactions, which use surface plasmon resonance technique,[5,6] high-speed capillary electrophoresis,[7] flow cytometry,[8] mass spectrometry,[9] fluorescence spectroscopy/imaging,[10,11] or the yeast two-hybrid system.[12] Among them, the fluorescence spectroscopy/imaging technique is a powerful tool for monitoring biological events by virtue of its high sensitivity, excellent temporal resolution, and good reproducibility.[13−15] The currently available fluorescent approaches to study protein–peptide interactions are largely based on green fluorescent protein,[16] fluorophore/quencher dual-labeled peptides,[17−19] or quencher/fluorophore-labeled peptide complex.[20] The requirement of dual modification of peptides or the use of complexes adds to the cost and complexity of the probe design and assay operation. In addition, most of the existing fluorescence assays for a protein–peptide interaction study do not operate in living organisms. Simple fluorescent probe design with improved properties remains in urgent pursuit for studying protein–peptide interactions, especially in living organisms.

More recently, a simple strategy for designing fluorescent light-up probes without any quencher molecules has been developed by taking advantage of fluorophores with intrinsic fluorescence activation mechanisms.[21−31] For instance, probes containing

* Address correspondence to cheliub@nus.edu.sg (B. Liu), yangzm@nankai.edu.cn (Z. M. Yang), dingd@nankai.edu.cn (D. Ding).

Received for review October 21, 2013 and accepted January 13, 2014.

Published online January 13, 2014
10.1021/nn4054914

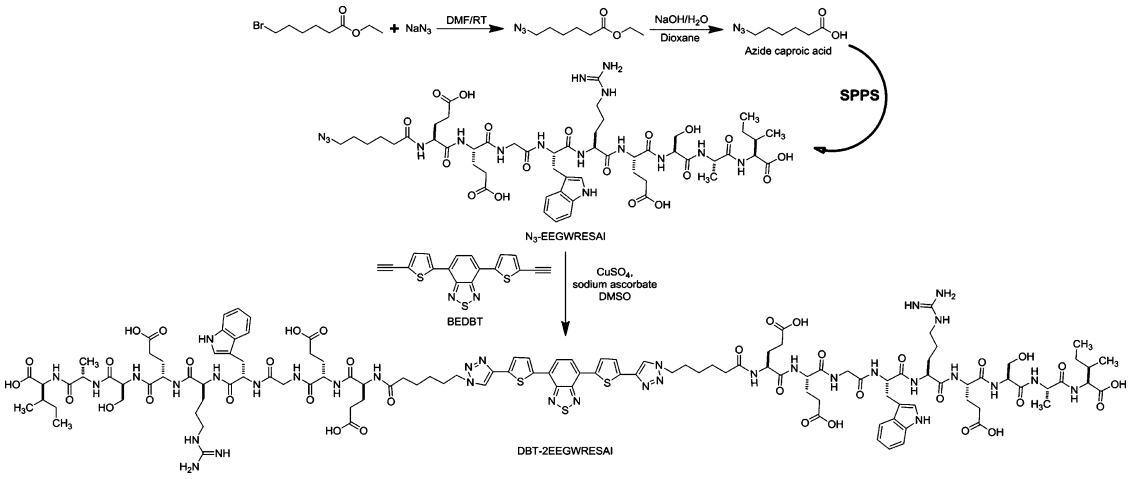

Scheme 1. Synthetic route to DBT-2EEGWRESAI probe.

fluorophores with aggregation-induced emission (AIE) characteristics or environment-sensitive molecules are often weakly fluorescent in aqueous media, while the fluorescence can be significantly switched on in the presence of target analytes. Traditional AIE fluorophores generally possess rotating units (*e.g.*, phenyl rings), which can turn on its fluorescence in aggregate state *via* a mechanism of restriction of intramolecular rotations (RIR).[24] On the other hand, the environment-sensitive fluorophores show weak fluorescence in polar environments due to the charge-transfer-induced fluorescence quenching but exhibit intense fluorescence in hydrophobic environments by reducing charge transfer between the fluorophore and polar media.[25−28] This light-up strategy has opened up new opportunities for the detection of biological events with high sensitivity and good signal-to-background ratios.[29−31] Most of the currently available fluorophores used in this strategy, however, are low-wavelength (*e.g.*, blue, green, yellow) emitters, while very few reports have been focused on fluorophores with far-red/near-infrared (FR/NIR) fluorescence.[32,33] It is well known that the FR/NIR region (650−900 nm) provides a unique window for bioimaging with minimal interferential absorption and low biological autofluorescence. FR/NIR fluorescent materials have shown great advantages in bioimaging and biosensing applications over those with short-wavelength emission.[34−37] To the best of our knowledge, there have been no previous reports on FR/NIR fluorescence turn-on probes without the aid of a quencher for visualization of protein−peptide interactions in solution and in living organisms.

In this contribution, we report the design and synthesis of an FR/NIR fluorescence light-up probe for specific detection and visualization of protein/polyprotein−peptide interactions. Tax-interacting protein-1 (TIP-1) and a fusion protein of ubiquitin-like domain (ULD) protein and TIP-1 (ULD-TIP-1) were chosen as model proteins. TIP-1 protein plays a key role in β-catenin transcriptional activity and growth of colorectal cancer cells, and we previously found that a hexapeptide ligand (WRESAI) can specifically bind to TIP-1 with high affinity.[38] Moreover, ULD protein can spontaneously form a tetramer, making ULD-TIP-1 appear as a polyprotein with four binding sites to peptides.[39] As protein aggregation is associated with several diseases such as Alzheimer's and Prion diseases,[40,41] detection of polyprotein and polyprotein−peptide interactions is of vital importance. In this work, the ULD-TIP-1 tetramer was used as a model polyprotein to assess the feasibility of our probe for detection of polyprotein−peptide interactions. We first synthesized 4,7-di(thiophen-2-yl)-2,1,3-benzothiadiazole (DBT) and demonstrated that DBT is an FR/NIR fluorogen with charge transfer excited states, which is sensitive to external environment. The FR/NIR fluorescence light-up probe (Scheme 1) was then synthesized by simply integrating two TIP-1-specific peptide ligands (EEGWRESAI) with one bisethynyl (BE)-functionalized DBT (BEDBT) unit *via* "click" chemistry. The probe (DBT-2EEGWRESAI) is water-soluble and almost non-fluorescent in aqueous environment. By virtue of the self-assembly between the TIP-1 or ULD-TIP-1 tetramer and the probe, DBT-2EEGWRESAI turns on its FR/NIR fluorescence, which is capable of detecting and visualizing specific protein/polyprotein−peptide interactions in both solution and live bacteria. As compared to the reported fluorescence-sensing approaches for studying protein−peptide interactions or protein detection, the uniqueness of our probe design includes (1) self-assembly-induced fluorescence turn-on mechanism favoring high fluorescence signal output; (2) two peptide ligands per DBT unit facilitating polyprotein−peptide interactions; (3) simple design of FR/NIR fluorescence light-up probes without the aid of quenchers; and (4) the ability to visualize protein/polyprotein−peptide interactions in live bacteria.

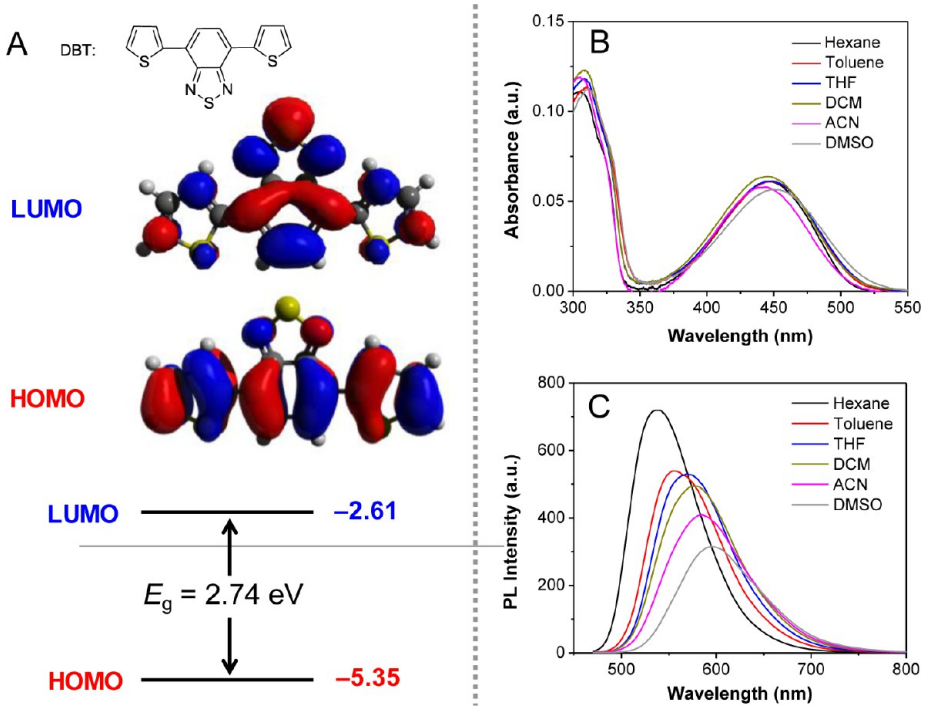

Figure 1. (A) Chemical structure and the frontier molecular HOMO and LUMO orbitals of DBT. (B) UV–vis absorption and (C) photoluminescence (PL) spectra of DBT in different solvents.

RESULTS AND DISCUSSION

To synthesize the FR/NIR fluorescence light-up probe, we started with the synthesis and characterization of DBT. We then carried out density functional theory calculation of DBT using a suite of the Gaussian 03 program to understand its properties at the molecular level. The nonlocal density functional of B3LYP with 6-31G(d) basis sets was used for the calculation. As shown in Figure 1A, the lowest unoccupied molecular orbital (LUMO) of DBT is dominated by the orbitals from the benzothiadiazole moiety, while the electron clouds of the highest occupied molecular orbital (HOMO) are mainly located on both the thiophenyl and benzothiadiazole moieties. The difference in electron cloud distribution shows intrinsic intramolecular electron transfer (ICT) character, which is beneficial to red-shifted emission spectra in polar media. This is further confirmed by the similar absorption spectra (Figure 1B) and red-shifted emission spectra (Figure 1C) in solvents of increasing polarity. This together with the decreased fluorescence intensity for DBT in more polar solvents reveals that DBT is an environment-sensitive fluorophore with FR/NIR fluorescence due to its strong charge transfer character in the excited state. We subsequently synthesized BEDBT with detailed synthesis and characterization in Scheme S1 and Figure S1 in the Supporting Information (SI). The synthetic route to DBT-2EEGWRESAI is depicted in Scheme 1. The azide-bearing EEGWRESAI peptide (N_3-EEGWRESAI) was prepared by standard solid-phase 9-fluorenylmethoxycarbonyl (Fmoc) peptide chemistry. Its ^{1}H NMR and HR-MS spectra are shown in Figures S2 and S3 in the SI. Subsequent coupling between BEDBT and the N_3-EEGWRESAI *via* a copper-catalyzed "click" reaction afforded the probe DBT-2EEGWRESAI in 86% yield. The purity and identity of the probe were characterized by HPLC, ^{1}H NMR, and MALDI-TOF-MS (Figures S4–S6 in the SI).

The UV–vis absorption spectrum of DBT-2EEGWRESAI in water is shown in Figure S7 in the SI. The DBT-2EEGWRESAI has an absorption maximum around 490 nm, which well matches the 488 nm laser excitation of confocal microscopy. The photoluminescence (PL) spectra of DBT-2EEGWRESAI in the absence and presence of TIP-1 protein are shown in Figure 2A. The DBT-2EEGWRESAI itself shows very weak fluorescence in water at various probe concentrations ranging from 6.7 to 300 μM (Figure S8 in the SI). It is noted that DBT-2EEGWRESAI itself cannot form any detectable nanostructures in aqueous solution by transmission electron microscopy (TEM) investigation, indicating that DBT-2EEGWRESAI is dissolved as molecular species.

The proposed principle of our probe DBT-2EEGWRESAI is illustrated in Scheme 2. By virtue of the good water solubility of the peptide, the DBT-2EEGWRESAI is miscible with water, which is almost nonfluorescent due to charge-transfer-induced fluorescence quenching in polar media (*cf.* Figure 2A). After introduction of a probe-specific protein, for example, TIP-1, the specific binding interactions between protein and peptide ligand will make the probe self-assemble into nanocomplexes. On the other hand, addition of

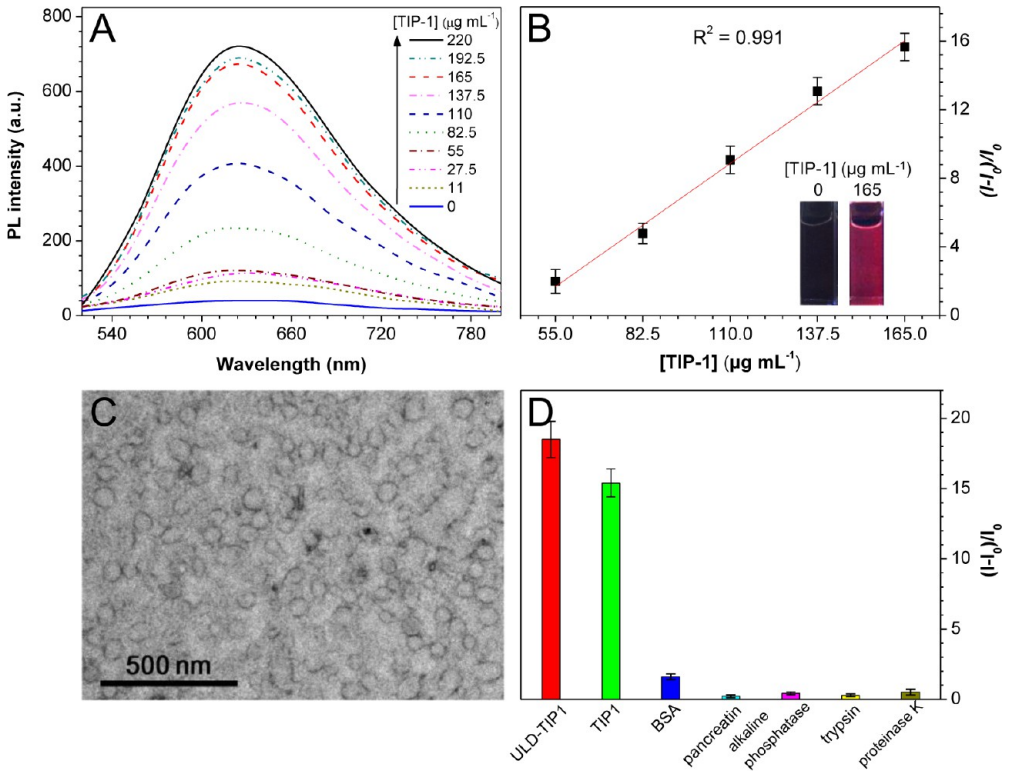

Figure 2. (A) PL spectra of DBT-2EEGWRESAI treated with different amounts of TIP-1. (B) Plot of $(I - I_0)/I_0$ *versus* concentration of TIP-1 in PBS buffer. I and I_0 are the PL intensities of DBT-2EEGWRESAI in the presence and absence of TIP-1, respectively. The data were expressed as mean ± standard deviation based on three measurements. Inset: Photographs taken under illumination of a UV lamp. (C) TEM image of DBT-2EEGWRESAI after treatment with 165 μg mL^{-1} of TIP-1. The nanocomplexes were negatively stained with uranyl acetate. (D) Plot of $(I - I_0)/I_0$ *versus* different proteins. I and I_0 are the PL intensities at protein concentrations of 165 and 0 μg mL^{-1}, respectively. [DBT-2EEGWRESAI] = 6.7 μM; λ_{ex} = 490 nm. The data are expressed as mean ± standard deviation based on four measurements.

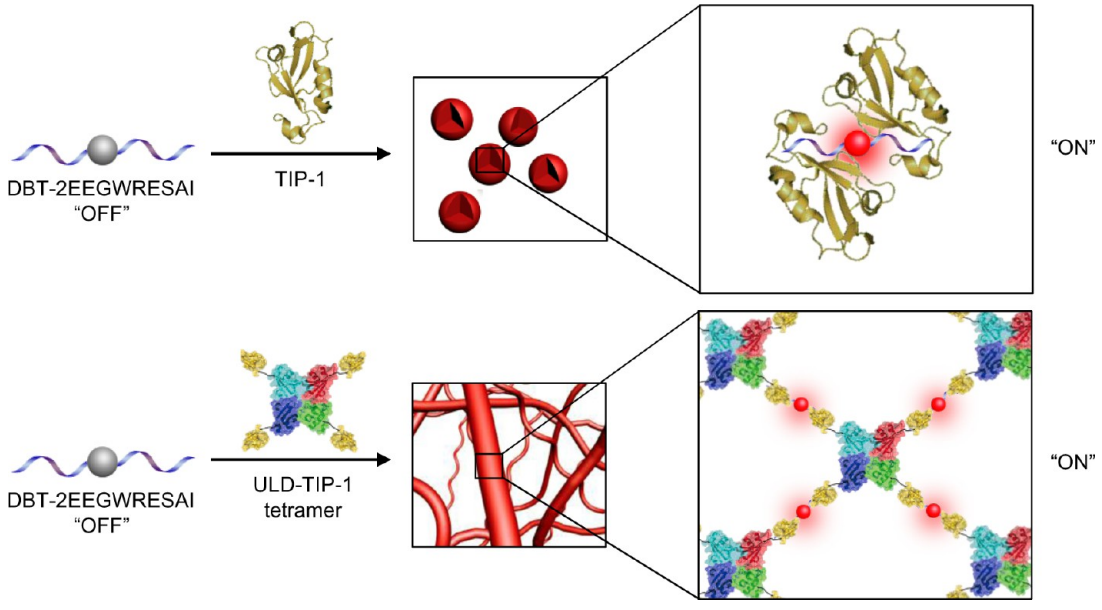

Scheme 2. Proposed principle of self-assembly-induced FR/NIR fluorescence light-up for detection and visualization of protein/polyprotein−peptide interactions based on DBT-2EEGWRESAI.

polyprotein (ULD-TIP-1 tetramer) into the probe aqueous solution may drive them to self-assemble into a nanofiber network through the interactions among four peptide binding sites of the ULD-TIP-1 tetramer and the two peptide ligands in each probe. Within these nanostructures, the microenvironmental hydrophobicity of DBT is expected to be significantly increased to lead to fluorescence light-up. In contrast,

when a protein possesses no specific interactions with DBT-2EEGWRESAI, no nanostructures would form, and the solution should remain dark.

To test the hypothesis, titration experiments were conducted by adding different amounts of TIP-1 protein into a DBT-2EEGWRESAI (6.7 μM) aqueous solution. As shown in Figure 2A, upon TIP-1 addition, the fluorescence of DBT-2EEGWRESAI is significantly switched on with an emission maximum at ~630 nm and an emission tail extending to 850 nm, allowing for FR/NIR fluorescence bioimaging and biosensing. Additionally, the DBT-2EEGWRESAI emission progressively increases with the increasing concentration of TIP-1. A ~18-fold increase in fluorescence is observed when the probe is treated with 165 μg mL^{-1} of TIP-1 in comparison to that of the same amount of probe alone. A plot of the net changes in fluorescence intensity against the TIP-1 concentration ranging from 55 to 165 μg mL^{-1} gives a good linear line (Figure 2B; full spectra are shown in Figure S9 in the SI), indicating the possibility of using DBT-2EEGWRESAI for TIP-1 quantification. Figure 2C shows the TEM image of DBT-2EEGWRESAI after incubation with TIP-1, which reveals that the DBT-2EEGWRESAI specifically binds to TIP-1 to yield nanocomplexes with a nearly spherical shape. The formed nanocomplexes should endow DBT with a hydrophobic microenvironment, reducing the charge transfer between DBT and the polar aqueous media, which is favorable to fluorescence turn-on as depicted in Scheme 2. Therefore, the fluorescence light-up mechanism of DBT-2EEGWRESAI is different from the RIR mechanism of AIE-based probes.

To demonstrate the probe selectivity, DBT-2EEGWRESAI was treated with several proteins including bovine serum albumin, pancreatin, alkaline phosphatase, trypsin, proteinase K, TIP-1 and ULD-TIP-1, under identical conditions. As shown in Figure 2D, TIP-1 and ULD-TIP-1 exhibit around 10- to 80-fold and 11- to 90-fold larger changes in $(I - I_0)/I_0$ as compared to five other proteins, respectively, revealing that DBT-2EEGWRESAI can serve as a unique probe for specific protein–peptide interaction detection.

We have previously demonstrated that TIP-1 and ULD-TIP-1 proteins could be expressed in *Escherichia coli*,[38,39] which allows us to study the application of DBT-2EEGWRESAI in detecting and visualizing protein/polyprotein–peptide interactions in live bacteria. The SDS-PAGE gel result reveals that the TIP-1 protein can be expressed in *E. coli* after inducing with isopropyl-β-D-thiogalactoside. As shown in Figure S10 in the SI, the expression level of TIP-1 is gradually increased over time, which saturates at around 3 h under the studied conditions. To detect protein–peptide interactions in bacteria, the *E. coli* were induced for TIP-1 expression and incubated with DBT-2EEGWRESAI at the same time in culture medium. After designated time intervals, the bacteria were centrifuged to remove the traces of free

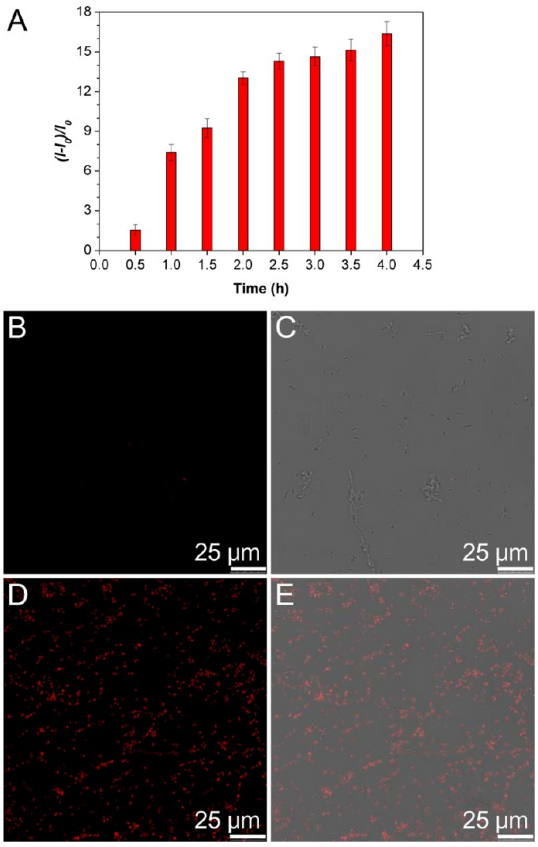

Figure 3. (A) Plot of $(I - I_0)/I_0$ *versus* TIP-1 expression/probe incubation times. I and I_0 are the fluorescence intensities of DBT-2EEGWRESAI in the presence and absence of bacteria, respectively. TIP-1 expression and probe incubation were carried out at the same time. The data were expressed as mean ± standard deviation based on three measurements. Confocal images of live bacteria after TIP-1 expression and probe incubation for (B) 0.5 and (D) 4 h. (C, E) Corresponding fluorescence/transmission overlay images of (B) and (D).

probes without bacterium uptake. The probe-treated bacteria were then lysed, and the bacterium lysates at different time points were collected for fluorescence measurement. As shown in Figure 3A, the net change in fluorescence intensity of the bacterium lysates enhances as the time elapses, which nearly reaches a plateau at around 3 h post protein expression. This is in agreement with the TIP-1 expression profile in *E. coli* shown in Figure S10 in the SI. As a control, no fluorescence increase is observed in the bacteria without inducing TIP-1 expression under the same experimental conditions within 4 h probe incubation. These data indicate that DBT-2EEGWRESAI is able to monitor specific protein–peptide interactions in bacteria.

We next investigated whether DBT-2EEGWRESAI is capable of visualizing the specific protein–peptide interactions in live bacteria. Figure 3B and C as well as Figure 3D and E show the confocal images of live *E. coli* after inducing TIP-1 expression along with incubation of DBT-2EEGWRESAI in culture medium for 0.5 and 4 h, respectively. These images were taken upon excitation at 488 nm with a 650 nm long-pass barrier filter.

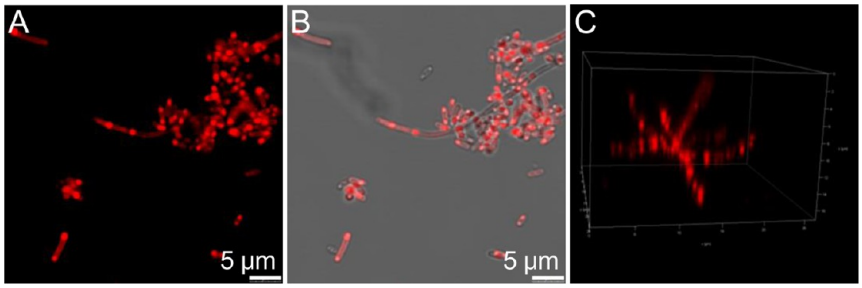

Figure 4. (A) Enlarged confocal image of live bacteria after TIP-1 expression and probe incubation for 4 h. (B) Corresponding fluorescence/transmission overlay image of (A). (C) 3D confocal image of DBT-2EEGWRESAI-stained live bacteria at 4 h.

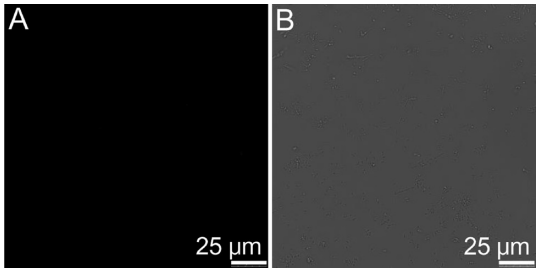

Figure 5. (A) Confocal images of live bacteria without inducing TIP-1 expression after incubation with DBT-2EEGWRESAI for 4 h. (B) Corresponding fluorescence/transmission overlay image of (A).

It is obvious that only a few fluorescent dots with relatively low brightness are observed at 0.5 h (Figure 3B and C), while strong fluorescence from the live bacteria is observed at 4 h, lighting up the TIP-1 proteins due to specific protein–peptide interactions (Figure 3D and E). The imaging results are consistent with those in Figures 3A and S10 in the SI as well. The enlarged images (Figure 4A and B) and the 3D confocal image (Figure 4C) of the probe-stained bacteria at 4 h further verify that the fluorescence is mainly from the interior of the bacteria. In comparison, under the same imaging conditions, almost no detectable fluorescence is observed for the control bacteria upon incubation with the same amount of probe for 4 h but without inducing TIP-1 expression (Figure 5). Moreover, as another control, DBT itself is not able to stain the live bacteria with and without inducing TIP-1 expression (Figure S11 in the SI). These results substantiate that DBT-2EEGWRESAI can be used to visualize specific protein–peptide interactions in live bacteria. Moreover, the probe does not show obvious cytotoxicity to the protein-expressed bacteria (Figure S12 in the SI), suggesting that DBT-2EEGWRESAI is a safe probe for imaging.

Although detection and visualization of polyprotein–peptide interactions could provide scientists with insight into the therapeutics of many diseases,[40] limited work has been focused on the fluorescent probes for such application. In this study, the ULD-TIP-1 tetramer was employed as a model polyprotein. Figure 6A shows the variation in the PL spectra of DBT-2EEGWRESAI (6.7 μM) upon addition of different amounts of ULD-TIP-1. At 165 μg mL^{-1} of ULD-TIP-1, the FR/NIR fluorescence of the probe is dramatically turned on to a maximum intensity that is ~20-fold stronger than that of the probe alone. As expected, the ULD-TIP-1 tetramer and DBT-2EEGWRESAI can self-assemble into a nanofiber network (Figure 6B), which stems from the multiple interactions among four peptide binding sites of the ULD-TIP-1 tetramer and two peptide ligands of DBT-2EEGWRESAI. In addition, the PL intensities of DBT-2EEGWRESAI after treatment with ULD-TIP-1 increase linearly with the increasing of protein concentrations from 0 to 110 μg mL^{-1} (Figure 6C). Furthermore, DBT-2EEGWRESAI can also significantly light up the ULD-TIP-1 tetramer in live *E. coli* (Figure 7). To confirm the ULD-TIP-1 tetramer/DBT-2EEGWRESAI interactions in bacteria, we broke the probe-stained bacteria and observed the formed nanofibers (Figure 8), which have a similar morphology to those formed by ULD-TIP-1 tetramer/DBT-2EEGWRESAI in aqueous solution (Figure 6B). In comparison, under the same experimental conditions, both the ULD-TIP-1-expressed bacteria alone and noninduced bacteria incubated with DBT-2EEGWRESAI do not show nanofiber formation. These data illustrate the ability and mechanism of DBT-2EEGWRESAI to visualize polyprotein–peptide interactions in live bacteria.

CONCLUSIONS

In summary, we developed an FR/NIR fluorescence light-up probe for detecting and visualizing specific protein/polyprotein–peptide interactions in both solution and live bacteria. Thanks to its environmental selectivity, DBT-2EEGWRESAI is very weakly fluorescent in aqueous solution but emits intensely upon specifically binding to TIP-1 or ULD-TIP-1 tetramer. The self-assemblies of DBT-2EEGWRESAI/TIP-1 and DBT-2EEGWRESAI/ULD-TIP-1 tetramer yield spherical nanocomplexes and a nanofiber network, respectively, which endow DBT with a hydrophobic microenvironment to induce fluorescence turn-on. The imaging experiments using protein-expressed bacteria reveal that DBT-2EEGWRESAI can serve as a unique probe for visualizing protein/polyprotein–peptide interactions in live bacteria. Its FR/NIR fluorescence makes the probe very promising for further bioimaging and biosensing

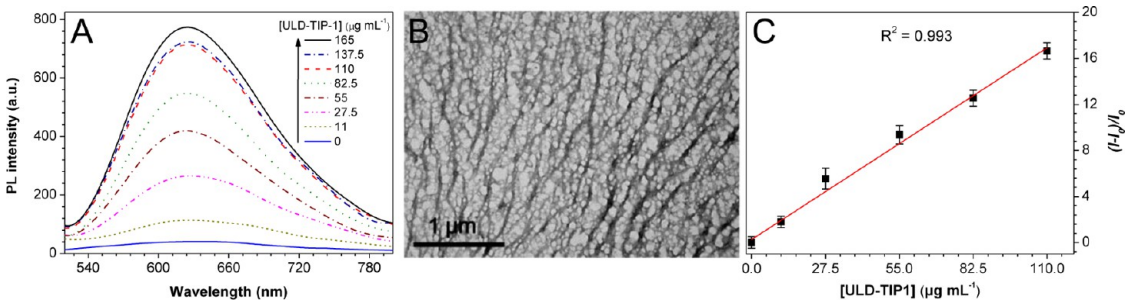

Figure 6. (A) PL spectra of DBT-2EEGWRESAI treated with different amounts of ULD-TIP-1. [DBT-2EEGWRESAI] = 6.7 μM; λ_{ex} = 490 nm. (B) TEM image of DBT-2EEGWRESAI after treatment with 165 μg mL^{-1} of ULD-TIP-1. (C) Plot of $(I - I_0)/I_0$ *versus* concentration of ULD-TIP-1 in PBS buffer. I and I_0 are the PL intensities of DBT-2EEGWRESAI in the presence and absence of ULD-TIP-1, respectively. The data are expressed as mean ± standard deviation based on three measurements.

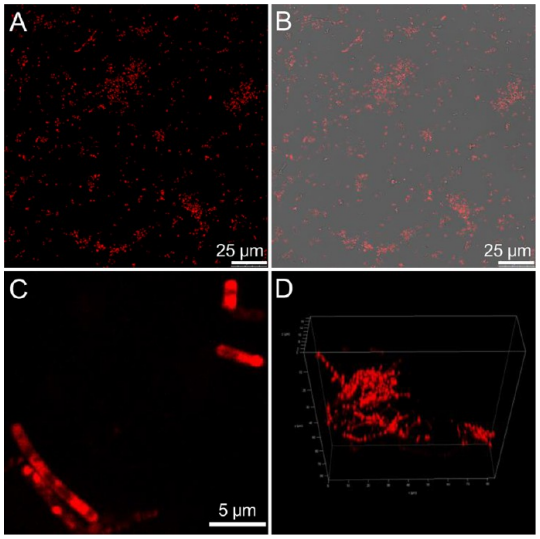

Figure 7. (A) Confocal image and (B) the corresponding fluorescence/transmission overlay image of live bacteria after ULD-TIP-1 expression and probe incubation for 4 h. (C) Enlarged confocal image and (D) 3D confocal image of DBT-2EEGWRESAI-stained live bacteria at 4 h.

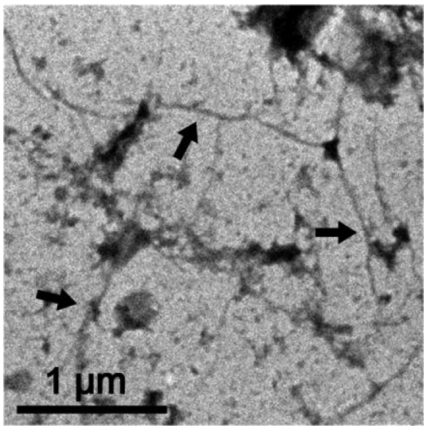

Figure 8. TEM image of the nanofibers formed in the bacteria. Arrows indicate the nanofibers.

applications. In light of its simplicity and high effectiveness, replacing EEGWRESAI with other peptide ligands could afford a series of FR/NIR fluorescent probes for studying other specific protein/polyprotein–peptide interactions. Furthermore, due to the special design of two peptide ligands per DBT unit, the resulting FR/NIR fluorescence light-up probes are capable of detecting polyprotein and polyprotein–peptide interactions, which would have important medical applications such as in diagnosing Alzheimer's and Prion diseases, which are associated with protein aggregation. This study thus provides fundamental guidelines to yield FR/NIR fluorescence light-up probes that hold great promise for clinical disease diagnostics.

EXPERIMENTAL SECTION

Materials. Fmoc-OSu and other Fmoc-amino acids were obtained from GL Biochem (Shanghai, China). 2-Cl-trityl chloride resin (1.0–1.2 mmol/g) was obtained from Nankai University Resin Co. Ltd. All the other starting materials were obtained from Alfa. Chemical reagents and solvents were used as received from commercial sources. 4,7-Di(thiophen-2-yl)-2,1,3-benzothiadiazole (DBT) was prepared according to a previous report.[42]

Characterization. ^{1}H NMR spectra were measured on a Bruker ARX 400. High-resolution mass spectra (HR-MS) were received from a VG ZAB-HS system (England). High-pressure liquid chromatography (HPLC) was carried out at a LUMTECH HPLC (Germany) system using a C_{18} RP column with MeOH (0.1% of TFA) and water (0.1% of TFA) as the eluents. UV–vis spectra were recorded on a Shimadzu UV-1700 spectrometer. Photoluminescence spectra were recorded on a Perkin-Elmer LS 55 spectrofluorometer. The morphology of the samples was studied by transmission electron microscopy (JEM-2010F, JEOL, Japan).

Synthesis of 4,7-Bis(5-bromothiophen-2-yl)-2,1,3-benzothiadiazole (DBT-Br). DBT-Br was synthesized according to a previous report with a modified procedure.[42] In brief, to a solution of DBT (0.90 g, 3.0 mmol) in *N*,*N*′-dimethylformamide (DMF, 50 mL) was slowly added *N*-bromosuccinimide (1.08 g, 6.1 mmol). After the reaction was carried out in the dark at room temperature for 3 h, water (150 mL) was added to give a red precipitate. The crude product was further purified by recrystallization from methanol to afford DBT-Br as bright red needles (1.1 g, yield: 81%). ^{1}H NMR (400 MHz, $CDCl_3$, ppm) δ: 7.81 (d, J = 4 Hz, 2 H), 7.78 (s, 2 H), 7.15 (d, J = 4 Hz, 2 H).

Synthesis of 4,7-Bis(5-ethynylthiophen-2-yl)benzothiadiazole (BEDBT). To a solution of DBT-Br (229.0 mg, 0.5 mmol), copper iodide (9.5 mg,

0.05 mmol), and $Pd(PPh_3)_2Cl_2$ (35.1 mg, 0.05 mmol) in diisopropylamine (30 mL) under an argon atmosphere was added ethynyltrimethylsilane (420 μL, 3.0 mmol) *via* syringe. The reaction was performed at 70 °C overnight before the solvent was removed under reduced pressure. The residue was redissolved in dichloromethane (DCM, 100 mL) and run through a short silica gel column to remove the catalyst. The crude product was mixed with potassium hydroxide (0.56 g, 10 mmol), THF (20 mL), methanol (10 mL), and water (5 mL) in a round bottle flask. The mixture was stirred at room temperature under an argon atmosphere for 1 h. After solvent removal, the residue was subsequently redissolved in DCM, washed with water, and dried over $MgSO_4$. The crude product was purified by silica gel column chromatography using hexane/DCM (v/v = 8/2) as eluent to afford BEDBT as a red solid (140.9 mg, yield: 81%). ^{1}H NMR (400 MHz, $CDCl_3$, ppm), δ: 7.95 (d, J = 6 Hz, 2 H), 7.82 (s, 2 H), 7.36 (d, J = 6 Hz, 2 H), 3.49 (s, 2 H). ^{13}C NMR (100 MHz, $CDCl_3$, ppm) δ: 152.3, 140.6, 133.9, 127.1, 125.7, 125.6, 123.4, 83.1, 77.2.

Synthesis of Azide Caproic Acid. Ethyl 2-bromohexanoate (2 g, 8.96 mmol) was dissolved in 8 mL of anhydrous DMF, which was followed by addition of sodium azide (0.84 g, 12.9 mmol). After stirring at room temperature for 14 h, 500 mL of petroleum ether was added into the system. The product was extracted by water three times and dried over anhydrous $MgSO_4$. The solvent was subsequently removed by rotary evaporator.

To obtain azide caproic acid, the crude product was dissolved in 4 mL of dioxane, which was followed by adding 4 mL of aqueous sodium hydroxide (21 wt %). After the mixture was reacted at 60 °C for 2 h, the solvent was removed by rotary evaporator. Subsequently, 2 M hydrochloric acid was added to the above aqueous solution to adjust the pH to ~3. The solution was then diluted with 500 mL of DCM and washed with water three times. The organic phase was combined and dried over anhydrous $MgSO_4$, which was followed by removal of solvent by rotary evaporator. The final product was obtained in 93.5% yield. The product was used for Fmoc solid-phase peptide synthesis without further purification.

Peptide Synthesis. The azide-bearing EEGWRESAI peptide (N_3-EEGWRESAI) was prepared by standard Fmoc solid-phase peptide synthesis (SPPS) using 2-chlorotrityl chloride resin and the corresponding N-Fmoc-protected amino acids with side chains properly protected by a *tert*-butyl group. Azide caproic acid was used as an amino acid. The growth of the peptide chain was according to the established Fmoc SPPS protocol. The obtained product was purified by HPLC. ^{1}H NMR (400 MHz, DMSO-d_6, ppm) δ: 7.60 (d, J = 7.8 Hz, 1 H), 7.45–7.52 (m, 1 H), 7.31 (d, J = 8.1 Hz, 1 H), 7.14 (s, 1 H), 7.08–7.00 (t, 1 H), 6.97 (t, J = 7.4 Hz, 1 H), 4.91 (s, 1 H), 4.64–4.53 (m, 1 H), 4.42–4.19 (m, 5 H), 4.14 (dd, J = 8.2, 6.0 Hz, 1 H), 3.76–3.51 (m, 6 H), 3.30–3.25 (m, 3 H), 3.18–3.05 (m, 2 H), 2.93 (dd, J = 14.8, 9.0 Hz, 1 H), 2.71–7.64 (m, 1 H), 2.54 (s, 2 H), 2.36–2.19 (m, 5 H), 2.18–2.08 (m, 2 H), 1.99–1.83 (m, 3 H), 1.83–1.66 (m, 4 H), 1.61–1.35 (m, 7 H), 1.33–1.12 (m, 5 H), 0.89–0.80 (m, 4 H). MS: calcd M^+ = 1214.5680, obsvd $(M + H)^+$ = 1215.5731.

Synthesis of DBT-2EEGWRESAI. An excess amount of N_3-EEGWRESAI (10 mg, 8.2 μmol) and BEDBT (1 mg, 2.9 μmol) were dissolved in 2 mL of dimethyl sulfoxide (DMSO). The click reaction was initiated by subsequent addition of 50 μL of 0.1 M $CuSO_4$ and 50 μL of 1 M sodium ascorbate aqueous solution. The reaction was allowed to proceed at room temperature under stirring for 16 h. The final product was purified by HPLC and obtained in 86% yield. ^{1}H NMR (400 MHz, DMSO-d_6, ppm) δ: 8.21–7.9 (m, 14 H), 7.62–7.51 (m, 1 H), 7.35–7.16 (m, 8 H), 7.15–6.92 (m, 11 H), 4.62–4.51 (m, 3 H), 4.47–4.20 (m, 12 H), 4.15–4.06 (m, 2 H), 3.75–3.56 (m, 13 H), 3.16–3.05 (m, 4 H), 2.90–2.65 (m, 10 H), 2.60–2.54 (m, 12 H), 2.35–2.10 (m, 10 H), 2.05–1.83 (m, 7 H), 1.82–1.63 (m, 6 H), 1.62–1.35 (m, 9 H), 1.32–1.10 (m, 9 H), 0.90–0.75 (m, 6 H). MS: calcd M^+ = 2778.1234, obsvd $(M + H)^+$ = 2779.1472.

Protein Expression and Purification. TIP-1 and ULD-TIP-1 proteins were expressed and purified using standard recombinant protein technology as previously reported.[38,39] In brief, DNA fragments corresponding to protein sequences were cloned into an in-house modified version of the pET32a (Novagen) in which the S-tag and the thrombin recognition site were replaced with a sequence encoding a PreScission protease-cleavable segment (Leu-Glu-Val-Leu-Phe-Gln-Gly-Pro). The resulting protein contained a Trx-His_6-tag in its N-terminus.

BL21(DE3) CodonPlus *E. coli* cells harboring the expression plasmid were grown in LB medium at 37 °C until the OD_{600} reached 0.6 and then induced with 0.3 mM isopropyl-β-D-thiogalactoside at 16 °C for about 16–18 h. Then collected *E. coli* cells *via* centrifugating were resuspended in $T_{50}N_{500}I_5$ buffer (50 mM Tris-HCl pH 7.9, 500 mM NaCl, and 5 mM imidazole) supplemented with 1 mM phenylmethylsulfonyl fluoride, 1 μg/mL leupeptin, and 1 μg/mL antipain. The cells were then lysed by sonication. After the lysates had been centrifuged, the supernatant was loaded onto a Ni-NTA agarose column (Qiagen) and a size-exclusion column (GE Healthcare). After digestion with PreScission protease to cleave the N-terminal Trx-His_6-tag, the target protein was purified on a Hiprep Q FF 16/10 anion-exchange column. The final purification step was size-exclusion chromatography on a HiLoad 26/60 Superdex 200 column in 100 mM PBS pH 7.4 and 100 mM NaCl. Typical protein yields were 70–130 mg from a one-liter cell culture.

Imaging in Live Bacteria. Single colonies of *E. coli* (BL21α, transformed with plasmid PET-32M-3C) on solid Luria–Bertani (LB) plates were transferred to 5 mL of liquid LB culture medium and were allowed to grow at 37 °C. When the value of OD_{600} reached 0.6, the bacteria were induced for protein expression by addition of 0.3 mM isopropyl-β-D-thiogalactoside at 16 °C. At the same time, the bacteria were also incubated with DBT-2EEGWRESAI in LB medium at the probe concentration of 9 μM. At the designated time intervals, the bacteria were harvested by centrifuging (5000 rpm for 1 min) and washed with 1× PBS three times. The supernatant was discarded, and the remaining bacteria were resuspended in 15 μL of 1× PBS buffer. Subsequently, the bacteria cells were spotted on glass slides and immobilized by the coverslips. The imaging tests were conducted on a Leica TSC SP8 confocal laser scanning microscope. The images were captured with CFI VC 60× oil immersed optics, and the fluorescent signals were collected upon excitation at 488 nm with a 650 nm long-pass barrier filter.

Toxicity of DBT-2EEGWRESAI against Bacteria. After *E. coli* were grown to an OD_{600} of 0.2 in LB medium on test tubes, 10 μM DBT-2EEGWRESAI was added to each tube and incubated with the bacteria. At the designated time intervals, the OD_{600} value of each tube was measured. The bacteria without incubation with the probes were used as the control. The results were the average of three measurements.

Conflict of Interest: The authors declare no competing financial interest.

Acknowledgment. This work was supported by the National Basic Research Program of China (2011CB964903), the NSFC (81301311, 51222303, and 81220108015), the Singapore National Research Foundation (R-279-000-390-281), and Singapore-MIT Alliance for Research and Technology (SMART) Innovation Grant (R279-000-378-592).

Supporting Information Available: Scheme and figures depicting detailed synthesis and characterization of BEDBT, N_3-EEGWRESAI, and DBT-2EEGWRESAI, UV–vis absorption spectrum of DBT-2EEGWRESAI, PL spectra of DBT-2EEGWRESAI at various concentrations, full PL spectra of Figure 2B, SDS-PAGE of TIP-1 expression in bacteria, confocal images of bacteria incubated with DBT, as well as cytotoxicity of DBT-2EEGWRESAI against bacteria. This material is available free of charge *via* the Internet at http://pubs.acs.org.

REFERENCES AND NOTES

1. Norman, T. C.; Smith, D. L.; Sorger, P. K.; Drees, B. L.; O'Rourke, S. M.; Hughes, T. R.; Roberts, C. J.; Friend, S. H.; Fields, S.; Murray, A. W. Genetic Selection of Peptide Inhibitors of Biological Pathways. *Science* **1999**, *285*, 591–595.
2. Venkatraman, P.; Nguyen, T. T.; Sainlos, M.; Bilsel, O.; Chitta, S.; Imperiali, B.; Stern, L. J. Fluorogenic Probes for Monitoring Peptide Binding to Class II MHC Proteins in Living Cells. *Nat. Chem. Biol.* **2007**, *3*, 222–228.

3. Petsalaki, E.; Russell, R. B. Peptide-Mediated Interactions in Biological Systems: New Discoveries and Applications. *Curr. Opin. Biotechnol.* **2008**, *19*, 344–350.
4. Eildal, J. N. N.; Hultqvist, G.; Balle, T.; Stuhr-Hansen, N.; Padrah, S.; Gianni, S.; Strømgaard, K.; Jemth, P. Probing the Role of Backbone Hydrogen Bonds in Protein-Peptide Interactions by Amide-to-Ester Mutations. *J. Am. Chem. Soc.* **2013**, *135*, 12998–13007.
5. Boozer, C.; Kim, G.; Cong, S.; Guan, H.; Londergan, T. Looking towards Lable-Free Biomolecular Interaction Analysis in a High-Throughput Format: A Review of New Surface Plasmon. *Curr. Opin. Biotechnol.* **2006**, *17*, 400–405.
6. Cherif, B.; Roget, A.; Villiers, C. L.; Calemczuk, R.; Leroy, V.; Marche, P. N.; Livache, T.; Villiers, M. B. Clinically Related Protein-Peptide Interactions Monitored in Real Time on Novel Peptide Chips by Surface Plasmon Resonance Imaging. *Clin. Chem.* **2006**, *52*, 255–262.
7. Yang, P.; Whelan, R. J.; Mao, Y.; Lee, A. W. M.; Carter-Su, C.; Kennedy, R. T. Multiplexed Detection of Protein-Peptide Interaction and Inhibition Using Capillary Electrophoresis. *Anal. Chem.* **2007**, *79*, 1690–1695.
8. Simons, P. C.; Young, S. M.; Carter, M. B.; Waller, A.; Zhai, D.; Reed, J. C.; Edwards, B. S.; Sklar, L. A. Simultaneous *In Vitro* Molecular Screening of Protein-Peptide Interactions by Flow Cytometry, Using Six Bcl-2 Family Proteins as Examples. *Nat. Protoc.* **2011**, *6*, 943–952.
9. Tu, T.; Drägusanu, M.; Petre, B. A.; Rempel, D. L.; Przybylski, M.; Gross, M. L. Protein-Peptide Affinity Dtermination Using an H/D Exchange Dilution Strategy: Application to Antigen-Antibody Interactions. *J. Am. Soc. Mass Spectrom.* **2010**, *21*, 1660–1667.
10. Lawrence, D. S.; Wang, Q. Seeing Is Believing: Peptide-Based Fluorescent Sensors of Protein Tyrosine Kinase Activity. *ChemBioChem* **2007**, *8*, 373–378.
11. Wruss, J.; Pollheimer, P. D.; Meindl, I.; Reichel, A.; Schulze, K.; Schofberger, W.; Piehler, J.; Tampe, R.; Blaas, D.; Gruber, H. J. Conformation of Receptor Adopted upon Interaction with Virus Revealed by Site-Specific Fluorescence Quenchers and FRET Analysis. *J. Am. Chem. Soc.* **2009**, *131*, 5478–5482.
12. Yang, M.; Wu, Z.; Fields, S. Protein-Peptide Interactions Analyzed with the Yeast Two-Hybrid System. *Nucleic Acids Res.* **1995**, *23*, 1152–1156.
13. Sainlos, M.; Iskenderian, W. S.; Imperiali, B. A General Screening Strategy for Peptide-Based Fluorogenic Ligands: Probes for Dynamic Studies of PDZ Domain-Mediated Interactions. *J. Am. Chem. Soc.* **2009**, *131*, 6680–6682.
14. Nam, T.; Park, S.; Lee, S. Y.; Park, K.; Choi, K.; Song, I. C.; Han, M. H.; Leary, J. J.; Yuk, S. A.; Kwon, I. C.; *et al.* Tumor Targeting Chitosan Nanoparticles for Dual-Modality Optical/MR Cancer Imaging. *Bioconjugate Chem.* **2010**, *21*, 578–582.
15. Wu, C. F.; Bull, B.; Szymanski, C.; Christensen, K.; McNeill, J. Multicolor Conjugated Polymer Dots for Biological Fluorescence Imaging. *ACS Nano* **2008**, *2*, 2415–2423.
16. Magliery, T. J.; Wilson, C. G. M.; Pan, W.; Mishler, D.; Ghosh, I.; Hamilton, A. D.; Regan, L. Detecting Protein-Protein Interactions with a Green Fluorescent Protein Fragment Reassembly Trap: Scope and Mechanism. *J. Am. Chem. Soc.* **2005**, *127*, 146–157.
17. Neuweiler, H.; Schultz, A.; Vaiana, A. C.; Smith, J. C.; Kaul, S.; Wolfrum, J.; Sauer, M. Detection of Individual p53-Autoantibodies by Using Quenched Peptide-Based Molecular Probes. *Angew. Chem., Int. Ed.* **2002**, *41*, 4769–4773.
18. Kohn, J. E.; Plaxco, K. W. Engineering a Signal Transduction Mechanism for Protein-Based Biosensors. *Proc. Natl. Acad. Sci. U.S.A.* **2005**, *102*, 10841–10845.
19. Voss, S.; Fischer, R.; Jung, G.; Wiesmuller, K. H.; Brock, R. A Fluorescence-Based Synthetic LPS Sensor. *J. Am. Chem. Soc.* **2007**, *129*, 554–561.
20. Lu, C. H.; Li, J.; Zhang, X. L.; Zheng, A. X.; Yang, H. H.; Chen, X.; Chen, G. N. General Approach for Monitoring Peptide-Protein Interactions Based on Graphene-Peptide Complex. *Anal. Chem.* **2011**, *83*, 7276–7282.
21. Kobayashi, H.; Ogawa, M.; Alford, R.; Choyke, P. L.; Urano, Y. New Strategies for Fluorescent Probe Design in Medical Diagnostic Imaging. *Chem. Rev.* **2010**, *110*, 2620–2640.
22. Mizusawa, K.; Takaoka, Y.; Hamachi, I. Specific Cell Surface Protein Imaging by Extended Self-Assembling Fluorescent Turn-on Nanoprobes. *J. Am. Chem. Soc.* **2012**, *134*, 13386–13395.
23. Lee, M. H.; Kim, J. Y.; Han, J. H.; Bhuniya, S.; Sessler, J. L.; Kang, C.; Kim, J. S. Direct Fluorescence Monitoring of the Delivery and Cellular Uptake of a Cancer-Targeted RGD Peptide-Appended Naphthalimide Theragnostic Prodrug. *J. Am. Chem. Soc.* **2012**, *134*, 12668–12674.
24. Shi, H. B.; Liu, J. Z.; Geng, J. L.; Tang, B. Z.; Liu, B. Specific Detection of Integrin $\alpha_v\beta_3$ by Light-Up Bioprobe with Aggregation-Induced Emission Characteristics. *J. Am. Chem. Soc.* **2012**, *134*, 9569–9572.
25. Toutchkine, A.; Kraynov, V.; Hahn, K. Solvent-Sensitive Dyes to Report Protein Conformational Changes in Living Cells. *J. Am. Chem. Soc.* **2003**, *125*, 4132–4145.
26. Shults, M. D.; Imperiali, B. Versatile Fluorescence Probes of Protein Kinase Activity. *J. Am. Chem. Soc.* **2003**, *125*, 14248–14249.
27. Loving, G. S.; Sainlos, M.; Imperiali, B. Monitoring Protein Interactions and Dynamics with Solvatochromic Fluorophores. *Trends Biotechnol.* **2010**, *28*, 73–83.
28. Zhuang, Y. D.; Chiang, P. Y.; Wang, C. W.; Tan, K. T. Environment-Sensitive Fluorescence Turn-On Probes Targeting Hydrophobic Ligand-Binding Domains for Selective Protein Detection. *Angew. Chem., Int. Ed.* **2013**, *52*, 8124–8128.
29. Lavis, L. D.; Raines, R. T. Bright Ideas for Chemical Biology. *ACS Chem. Biol.* **2008**, *3*, 142–155.
30. Sakabe, M.; Asanuma, D.; Kamiya, M.; Iwatate, R. J.; Hanaoka, K.; Terai, T.; Nagano, T.; Urano, Y. Rational Design of Highly Sensitive Fluorescence Probes for Protease and Glycosidase Based on Precisely Controlled Spirocyclization. *J. Am. Chem. Soc.* **2013**, *135*, 409–414.
31. Gao, Y.; Shi, J. F.; Yuan, D.; Xu, B. Imaging Enzyme-Triggered Self-Assembly of Small Molecules Inside Live Cells. *Nat. Commun.* **2012**, *3*, 1033.
32. Nalbant, P.; Hodgson, L.; Kraynov, V.; Toutchkine, A.; Hahn, K. M. Activation of Endogenous Cdc42 Visualized in Living Cells. *Science* **2004**, *305*, 1615–1619.
33. MacNevin, C. J.; Gremyachinskiy, D.; Hsu, C. W.; Li, L.; Rougie, M.; Davis, T. T.; Hahn, K. M. Environment-Sensing Merocyanine Dyes for Live Cell Imaging Applications. *Bioconjugate Chem.* **2013**, *24*, 215–223.
34. Frangioni, J. V. *In Vivo* Near-Infrared Fluorescence Imaging. *Curr. Opin. Chem. Biol.* **2003**, *7*, 626–634.
35. Mohan, N.; Tzeng, Y. K.; Yang, L.; Chen, Y. Y.; Hui, Y. Y.; Fang, C. Y.; Chang, H. C. Sub-20-nm Fluorescent Nanodiamonds as Photostable Biolabels and Fluorescence Resonance Energy Transfer Donors. *Adv. Mater.* **2010**, *22*, 843–847.
36. Ding, D.; Li, K.; Qin, W.; Zhan, R. Y.; Hu, Y.; Liu, J. Z.; Tang, B. Z.; Liu, B. Conjugated Polymer Amplified Far-Red/Near-Infrared Fluorescence from Nanoparticles with Aggregation-Induced Emission Characteristics for Targeted *in Vivo* Imaging. *Adv. Healthcare Mater.* **2013**, *2*, 500–507.
37. Jin, Y. H.; Ye, F. M.; Zeigler, M.; Wu, C. F.; Chiu, D. T. Near-Infrared Fluorescent Dye-Doped Semiconducting Polymer Dots. *ACS Nano* **2011**, *5*, 1468–1475.
38. Yan, X. J.; Zhou, H.; Zhang, J. X.; Shi, C. W.; Xie, X. Q.; Wu, Y. N.; Tian, C. L.; Shen, Y. Q.; Long, J. F. Molecular Mechanism of Inward Rectifier Potassium Channel 2.3 Regulation by Tax-Interacting Protein-1. *J. Mol. Biol.* **2009**, *392*, 967–976.
39. Zhang, X. L.; Chu, X. L.; Wang, L.; Wang, H. M.; Liang, G. L.; Zhang, J. X.; Long, J. F.; Yang, Z. M. Rational Design of a Tetrameric Protein to Enhance Interactions between Self-Assembled Fibers Gives Molecular Hydrogels. *Angew. Chem., Int. Ed.* **2012**, *51*, 4388–4392.
40. Ross, C. A.; Poirier, M. A. Protein Aggregation and Neurodegenerative Disease. *Nat. Med.* **2004**, *10*, S10–S17.

41. Droumaguet, B. L.; Nicolas, J.; Brambilla, D.; Mura, S.; Maksimenko, A.; Kimpe, L. D.; Salvati, E.; Zona, C.; Airoldi, C.; Canovi, M.; *et al*. Versatile and Efficient Targeting Using a Single Nanoparticulate Platform: Application to Cancer and Alzheimer's Disease. *ACS Nano* **2012**, *6*, 5866–5879.
42. Hou, Q.; Xu, Y.; Yang, W.; Yuan, M.; Peng, J.; Cao, Y. Novel Red-Emitting Fluorene-Based Copolymers. *J. Mater. Chem.* **2002**, *12*, 2887–2892.